PHYSICAL REVIEW B **81**, 220301(R) (2010)

Temperature dependence of electron-phonon thermalization and its correlation to ultrafast magnetism

Xuan Wang, Shouhua Nie, Junjie Li, Richard Clinite, John Edward Clark, and Jianming Cao*
Physics Department and National High Magnetic Field Laboratory, Florida State University, Tallahassee, Florida 32310, USA
(Received 11 January 2010; revised manuscript received 27 February 2010; published 11 June 2010)

We report a systematic measurement of the electron-phonon thermalization time scale as a function of the sample base temperature in Ni using femtosecond electron diffraction. A strong temperature dependence of this time scale has been observed in the vicinity of the Curie point. By assuming that ultrafast magnetism completes well before the electron-phonon thermalization, this correlation between thermalization time and sample base temperature fits a modified three-temperature model describing the energy transfer among charge, spin, and phonon subsystems. The results indicate that charges and spins can be characterized by a unified temperature during ultrafast lattice heating.

DOI: 10.1103/PhysRevB.81.220301 PACS number(s): 63.20.kd, 71.36.+c

The ultrafast dynamics of itinerant ferromagnets induced by femtosecond (fs) optical excitation involving the mutual interactions among charge, spin, and lattice is one of the most challenging subjects encountered in the quest for a thorough understanding of magnetism in ferromagnets. Since the pioneering work on ultrafast magnetism by time-resolved magneto-optical Kerr effect in 1996,[1] many groups have observed subpicosecond quenching and subsequent recovery of the ferromagnetic order in nickel by using a variety of techniques.[2–7] In recent years, these studies have been extended to other ferromagnetic metals,[8–12] ferromagnetic semiconductors,[13,14] and more complicated magnetic compounds.[15–22]

One main issue in ultrafast magnetism is to understand the role and time scale of elementary scattering processes involving electrons and quasiparticles like magons and phonons. These elementary processes regulate the energy and angular moment exchanges among charge, spin, and lattice to rebuild a new thermal equilibrium. For ferromagnetic metals such as nickel, a phenomenological three-temperature model, modified from widely used two-temperature model (TTM)[23,24] was first developed to describe the energy flow among these three subsystems.[1] In this model, each subsystem is assumed internally thermalized and characterized by its own temperature. More recent studies reveal that the spin dynamics is also governed by the carrier temperature once a thermalized Fermi-Dirac distribution of carriers has been established.[3,9,25,26] This approach with a unified temperature for both carriers and spins implies a spin-relaxation rate comparable to momentum relaxation rate of carriers, which challenges the conventional spin-relaxation theory.[27]

So far, nearly all the experiments have been carried out using exclusively optical pump-probe methods to monitor the relaxation of the charge carriers and spins. On the other hand, direct measurements of dynamics in the lattice degree of freedom and its correlation to magnetic ordering are sparse.[4] In a system that encompasses strong couplings among spin, charge, and lattice, the state change in one subsystem, such as demagnetization in spins, could profoundly modify the time scale of subsequent process such as electron-phonon (e-ph) thermalization. This is particularly true in the vicinity of the Curie temperature where a strong temperature dependence of electron heat capacity exists due to the high-energy cost to break ferromagnetic ordering.[28]

Here, we report a systematic investigation of the electron-phonon coupling kinetics induced by fs laser excitation in nickel by using femtosecond electron diffraction (FED). In contrast to previous experiments, which were carried out either at room temperature or at low pumping fluence yielding only a small increase in the spin temperature far below its Curie point, this study was conducted under relatively high pump conditions at and near the sample Curie point. We have observed a strong temperature dependence of the lattice-heating time scale around the Curie point. This dependence can be reproduced by a simulation based on a modified TTM model that was suggested by previous studies.[3,9,25,26] These results provide a strong evidence of ultrafast magnetism and its impact on electron-phonon thermalization, thus addressing an open question whether the unified temperature model is still valid for a strong demagnetization near the Curie point.[6,29–31]

The experiments were conducted on a third-generation femtosecond electron diffraction instrument with an increased electron-beam energy up to 100 kV.[32] The electron-diffraction patterns were recorded with a two-dimensional single-electron detector.[33] To maintain optimal time resolution, the average electron-beam intensity was set to contain less than 1200 electrons per pulse. The overall temporal resolution was estimated to be less than 500 fs.[34,35]

The polycrystalline thin-film nickel samples with a thickness of 22 ± 4.0 nm measured with an atomic force microscopy, were prepared by sputtering nickel from a 99.99% purity target in high vacuum onto freshly cleaved NaCl single-crystal substrates. The films on NaCl substrates were subsequently detached in a solvent and transferred to TEM grids as free-standing films. The films on TEM grids were mounted on a heating/cooling sample holder inside the chamber with a base pressure better than 3×10^{-10} torr. In the FED measurements, the laser excitation fluences were set to 0.8 and 2.4 mJ/cm^2 in two sets of experiments and no sample damage was observed after extended exposure to the pump-laser pulses.

Structural dynamics of the nickel sample were initiated by fs optical excitation and recorded by capturing snapshots of

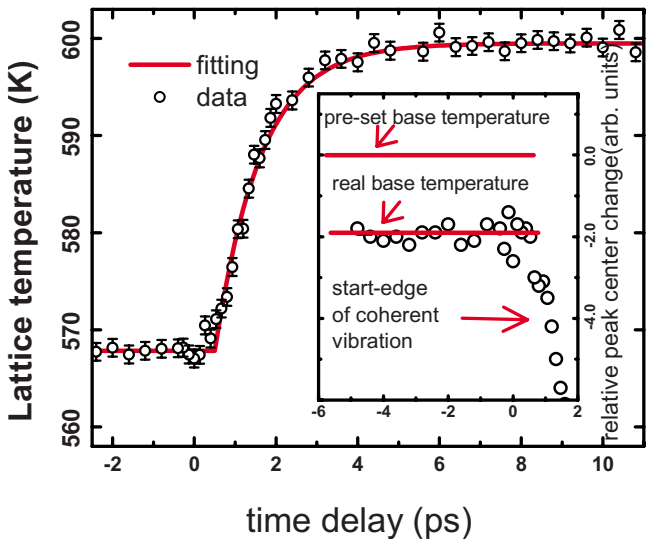

FIG. 1. (Color online) Temporal evolution of lattice temperature. The solid curve is a fit by Eq. (1). The solid line is a fit using monoexponential with a time constant 1.117 ± 0.074 ps. Inset: normalized Bragg-peak position change as a function of time. The normalized peak position is obtained by dividing the peak position with the laser on (with the residual heating and the laser-induced temperature jump) by that without laser excitation (at preset sample temperature). The corresponding Bragg-peak shift is shown as a thermal expansion relative to the preset sample temperature before time zero. The change in peak position after time zero is due to a coherent vibration along the surface normal of the nickel film.

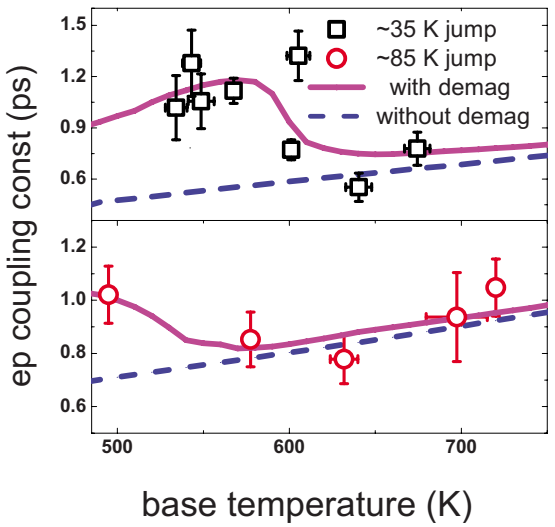

FIG. 2. (Color online) Time constant of electron-phonon thermalization as a function of sample base temperature at the vicinity of Curie point. The two-temperature jumps correspond to two different excitation fluencies. The solid curves are the simulation results with the assumption of ultrafast magnetization while the dashed curves are the ones assuming no ultrafast magnetization.

diffraction patterns at various pump-probe delay times. To obtain a quantitative measurement of structural changes, a recorded two-dimensional diffraction pattern was converted to a diffraction intensity curve as a function of diffraction angle θ (momentum transfer $S=2 \sin \theta/\lambda$).[32] Then, each Bragg peak in the intensity curve was fitted with a Gaussian line profile to determine its peak center (peak position), peak intensity, and the peak width. Finally the temporal evolution of the peak intensity curve was converted to temporal evolution of lattice temperature curve by applying a Debye-Waller factor, which was calibrated by measuring the static diffraction intensity as function of sample temperature. In the FED measurement, due to the residual heating of 1 kHz pump-laser pulses, the actual sample temperature before time zero (sample base temperature) is always higher than the preset stage temperature. This temperature shift due to the residual heating was determined by dividing the Bragg-peak center shift with the linear thermal-expansion coefficient (see inset of Fig. 1). In our experiments, the residual heating drastically increases the actual base temperature for about 50 K at low laser excitation and over 100 K at high laser excitation. However, this shift was found to be very stable for each data set with a fluctuation of 5 K.[36]

Figure 1 shows a typical temporal evolution of lattice temperature as a function of pump-probe delay time. The curve displays a monoexponential time dependence and can be well fitted by the equation,

$$\delta T_l = T_l^{\infty}(1 - e^{-(t-t_0)/\tau}), \tag{1}$$

where T_l^{∞} represents the overall temperature change in the lattice, t_0 is the time-zero point, and τ is the time constant of lattice heating. We also tracked this lattice temperature curve up to several hundred picoseconds and did not detect any further changes after ~ 10 ps. This indicates that the heating of nickel lattice is completed in less than 10 ps, eliminating the possibility of subsequent energy flow between spins and lattice. In addition, the observed monoexponential behavior implies that the spins and charges may be viewed as a single-energy "reservoir" characterized by a unified temperature when they are interacting with the lattice, in analogy to the electron-phonon coupling in noble metals. To further check this assumption, we measured the time constant of lattice heating as a function of sample base temperature under two different laser excitation fluencies in the vicinity of the Curie temperature T_c. A very distinct feature revealed by these measurements, as shown in Fig. 2, is a large increase in the lattice-heating time constants around the Curie point. This temperature dependence of lattice-heating time constant resembles very closely the shape of the overall electron heat-capacity changes (including magnetic contribution) in the vicinity of T_c,[28] indicating a strong modification of magnetic ordering. Such a jump becomes less prominent and also shifts its turning point toward the lower temperature at higher excitation fluences, as shown in Fig. 2(b).

Based on the previous studies at low fluence, we simulated the electron-phonon coupling time constants in the vicinity of T_c using a modified three-temperature model[1] by assuming that charge and magnetic subsystems can be characterized by a single and unified temperature T_{em}. This assumption presumes that the time required for energy transfer between the charge and the magnetic degrees of freedom is

comparable to that of electron thermalization, such that these two subsystems establish a thermal equilibrium around 100 fs and is characterized by an unified temperature T_{em}.[3,9,25] It is worth pointing out that in a recent experiment on nickel, the difference of thermalization time between carriers and spins have been clearly resolved.[37] However, since such difference is only tens of femtosecond, the assumption of an unified temperature T_{em} should still hold when considering the lattice thermalization of a few picosecond time scale. This T_{em} is initially higher than the lattice temperature T_l, thus driving the energy flow from electrons to lattice. Accordingly, the three-temperature model is reduced to the two-temperature model,

$$(C_e + C_m)\frac{\partial T_{em}}{\partial t} = -(G_{el} + G_{ml})(T_{em} - T_l) + S,$$

$$C_l\frac{\partial T_l}{\partial t} = +(G_{el} + G_{ml})(T_{em} - T_l), \tag{2}$$

where C_e, C_l, and C_m represent, respectively, the heat capacities of electrons, lattice, and magnetic ordering, G_{el} (G_{ml}) represents the coupling constant between electron (magnetic ordering) and lattice, and S represents the deposited laser-pulse energy of a Gaussian profile with 50 fs full width at half maximum. This pump-laser energy is absorbed by electrons without perturbing the magnetic ordering.

By assuming electrons and spins maintain a thermal equilibrium throughout the course of electron-phonon thermalization, we can introduce an effective e-ph coupling constant G_e as the sum of G_{el} and G_{ml} in the simulation. The G_e of nickel has been theoretically calculated as a function of electron temperature up to 4000 K,[38] which spans the temperature range in our experiment with a maximum T_e jump about 1000 K. In the calculation, a key parameter, $\lambda\langle w^2\rangle$, which characterizes the e-ph interaction, was extracted from a pump-probe reflectivity measurement of the carrier relaxation process[39] where the mutual interactions among the three subsystem, especially, the ultrafast magnetism were involved. Therefore, the calculated G_e by this $\lambda\langle w^2\rangle$ can be viewed as an effective overall coupling constant combining G_{el} and G_{ml}. In general, the value of G_e will decrease slightly with increasing electron temperature. Finally we take into account the energy cost of ultrafast demagnetization by plugging the experimental heat-capacity data of nickel in the relevant temperature range[28] and numerically solve the Eq. (2). The simulation results are plotted as solid curves in Fig. 2. As a comparison, we also simulate the lattice-heating dynamics without ultrafast magnetism (using same G_e but excluding C_m), which are plotted as dotted curves in Fig. 2. The simulation results with ultrafast magnetism reproduce the trend of the experimental data. In contrast, the results without ultrafast magnetism are significantly faster and increase monotonically with increasing temperature. These observations indicate that TTM with a unified temperature for charge and magnetic subsystems, rather than a more complicated but more general three-temperature model, is more suitable to describe the ultrafast lattice heating in ferromagnetic Ni.

The large increase in the e-ph coupling time constant around the Curie temperature reflects the large energy cost required to break magnetic ordering and is correlated with the large jump of electron heat capacity around the Curie point.[28] Due to this larger spin heat capacity, the laser-induced temperature increase in electrons becomes much smaller. Given that the overall coupling constant G_e does not change significantly, this drop in temperature difference between electrons and lattice will reduce the energy-flow rate between the two subsystems and thus elongate the time scale to build a new thermal equilibrium between them, as shown in Fig. 2. Since the abnormality of electron heat capacity is only confined in the vicinity of Curie point, a larger overall electron temperature jump induced by higher-power laser heating will tend to "smear-out" such lengthening effect, as shown in panel (b) of Fig. 2.

The subpicosecond magnetism in Ni revealed by direct and real-time monitoring of the ultrafast heating of the lattice using femtosecond electron diffraction provides a unique insight into the dynamics of ultrafast demagnetization from the aspect of energy flow in the correlated electron system. Our results together with other experimental and theoretical studies[2,3,9,25,40–42] all support a general picture that spin and electron systems share the same temperature following electron thermalization completed in a few hundred femtoseconds after optical excitation. This fast spin-relaxation process can be attributed to several intrinsic scattering mechanisms, including Stoner excitation,[2,42] electron-magnon excitation,[41] phonon-induced and phonon-mediated spin-flip events.[40,43,44] Recently, the photon-mediated spin-relaxation process[21,22,37,45] is attracting much attention due to its unique advantage of ultrafast and no overheating nature in magnetization reversal. Since photon field only persists in the duration of optical pulse length on a 100 fs or less time scale that is shorter than the entire course of ultrafast magnetism (quenching and possible recovering or switching of magnetic ordering), an intrinsic scattering mechanism is still needed to account for such a fast spin-relaxation process after the transient laser field. A simultaneous and real-time monitoring of all degrees of freedom involving charge, spin, lattice, and their mutual interactions might hold the key to finally unraveling the underlying mechanism of this ultrafast demagnetization.

In conclusion, we have studied the interaction dynamics among charge, spin, and lattice subsystems in ferromagnetic nickel using femtosecond electron diffraction. By measuring rates of energy transfer as a function of sample temperature in the vicinity of Curie point, we show that the demagnetization induced by fs optical excitation proceeds in a time scale much faster than the lattice heating in nickel. Meanwhile our results imply that such demagnetization is most likely completed within the time scale of electron thermalization so that one unified temperature for electrons and magnetic subsystems under TTM is adequate to describe ultrafast lattice heating in nickel.

The authors would like to thank P. Xiong and S. von Molnár for the use of their thin-film preparation equipment. This work was supported by NSF under Grant No. DMR-0907262.

*Author to whom correspondence should be addressed; jcao@magnet.fsu.edu

[1] E. Beaurepaire, J. C. Merle, A. Daunois, and J.-Y. Bigot, Phys. Rev. Lett. **76**, 4250 (1996).
[2] H. S. Rhie, H. A. Durr, and W. Eberhardt, Phys. Rev. Lett. **90**, 247201 (2003).
[3] J. Hohlfeld, E. Matthias, R. Knorren, and K. H. Bennemann, Phys. Rev. Lett. **78**, 4861 (1997).
[4] C. Stamm, T. Kachel, N. Pontius *et al.*, Nature Mater. **6**, 740 (2007).
[5] B. Koopmans, M. van Kampen, J. T. Kohlhepp, and W. J. M. de Jonge, Phys. Rev. Lett. **85**, 844 (2000).
[6] A. Scholl, L. Baumgarten, R. Jacquemin, and W. Eberhardt, Phys. Rev. Lett. **79**, 5146 (1997).
[7] M. van Kampen, C. Jozsa, J. T. Kohlhepp, P. LeClair, L. Lagae, W. J. M. de Jonge, and B. Koopmans, Phys. Rev. Lett. **88**, 227201 (2002).
[8] M. Lisowski, P. A. Loukakos, A. Melnikov, I. Radu, L. Ungureanu, M. Wolf, and U. Bovensiepen, Phys. Rev. Lett. **95**, 137402 (2005).
[9] J. Gudde, U. Conrad, V. Jahnke, J. Hohlfeld, and E. Matthias, Phys. Rev. B **59**, R6608 (1999).
[10] M. Cinchetti, M. Sánchez Albaneda, D. Hoffmann, T. Roth, J.-P. Wüstenberg, M. Krauß, O. Andreyev, H. C. Schneider, M. Bauer, and M. Aeschlimann, Phys. Rev. Lett. **97**, 177201 (2006).
[11] T. Kampfrath, R. G. Ulbrich, F. Leuenberger, M. Münzenberg, B. Sass, and W. Felsch, Phys. Rev. B **65**, 104429 (2002).
[12] M. Vomir, L. H. F. Andrade, L. Guidoni, E. Beaurepaire, and J.-Y. Bigot, Phys. Rev. Lett. **94**, 237601 (2005).
[13] A. Oiwa, Y. Mitsumori, R. Moriya, T. Slupinski, and H. Munekata, Phys. Rev. Lett. **88**, 137202 (2002).
[14] J. Wang, C. Sun, J. Kono, A. Oiwa, H. Munekata, Ł. Cywiński, and L. J. Sham, Phys. Rev. Lett. **95**, 167401 (2005).
[15] A. V. Kimel, R. V. Pisarev, J. Hohlfeld, and T. Rasing, Phys. Rev. Lett. **89**, 287401 (2002).
[16] T. Kise, T. Ogasawara, M. Ashida, Y. Tomioka, Y. Tokura, and M. Kuwata-Gonokami, Phys. Rev. Lett. **85**, 1986 (2000).
[17] R. D. Averitt and A. J. Taylor, J. Phys.: Condens. Matter **14**, R1357 (2002).
[18] U. Atxitia, O. Chubykalo-Fesenko, R. W. Chantrell, U. Nowak, and A. Rebei, Phys. Rev. Lett. **102**, 057203 (2009).
[19] G. Ju, A. V. Nurmikko, R. F. C. Farrow, R. F. Marks, M. J. Carey, and B. A. Gurney, Phys. Rev. Lett. **82**, 3705 (1999).
[20] G. Ju, J. Hohlfeld, B. Bergman, R. J. M. van de Veerdonk, O. N. Mryasov, J.-Y. Kim, X. Wu, D. Weller, and B. Koopmans, Phys. Rev. Lett. **93**, 197403 (2004).
[21] C. D. Stanciu, F. Hansteen, A. V. Kimel, A. Kirilyuk, A. Tsukamoto, A. Itoh, and T. Rasing, Phys. Rev. Lett. **99**, 047601 (2007).
[22] K. Vahaplar, A. M. Kalashnikova, A. V. Kimel, D. Hinzke, U. Nowak, R. Chantrell, A. Tsukamoto, A. Itoh, A. Kirilyuk, and T. Rasing, Phys. Rev. Lett. **103**, 117201 (2009).
[23] F. Vallée, C. R. Acad. Sci., Ser. IV Phys. Astrophys. **2**, 1469 (2001).
[24] P. B. Allen, Phys. Rev. Lett. **59**, 1460 (1987).
[25] L. Guidoni, E. Beaurepaire, and J.-Y. Bigot, Phys. Rev. Lett. **89**, 017401 (2002).
[26] T. Kachel, N. Pontius, C. Stamm, M. Wietstruk, E. F. Aziz, H. A. Dürr, W. Eberhardt, and F. M. F. de Groot, Phys. Rev. B **80**, 092404 (2009).
[27] R. J. Elliott, Phys. Rev. **96**, 266 (1954).
[28] P. J. Meschter, J. W. Wright, C. R. Brooks *et al.*, J. Phys. Chem. Solids **42**, 861 (1981).
[29] M. Djordjevic and M. Münzenberg, Phys. Rev. B **75**, 012404 (2007).
[30] U. Atxitia, O. Chubykalo-Fesenko, N. Kazantseva *et al.*, Appl. Phys. Lett. **91**, 232507 (2007).
[31] B. Koopmans, G. Malinowski, F. Dalla Longa *et al.*, Nature Mater. **9**, 259 (2010).
[32] X. Wang, S. Nie, J. Li *et al.*, Appl. Phys. Lett. **92**, 121918 (2008).
[33] J. Cao, Z. Hao, H. Park *et al.*, Appl. Phys. Lett. **83**, 1044 (2003).
[34] H. Park, X. Wang, S. Nie *et al.*, Solid State Commun. **136**, 559 (2005).
[35] X. Wang, S. Nie, H. Park *et al.*, Rev. Sci. Instrum. **80**, 013902 (2009).
[36] Residual heating depends on extrinsic sample conditions such as TEM grid size. More slim TEM grids are used to repeat the experiments at 567.6 K and 601 K (see Fig. 2). In this case, the residual heating reduces to less than 10 K with a fluctuation less than 1 K yielding a better S/N ratio.
[37] J. Y. Bigot, M. Vomir, and E. Beaurepaire, Nat. Phys. **5**, 515 (2009).
[38] Z. Lin, L. V. Zhigilei, and V. Celli, Phys. Rev. B **77**, 075133 (2008).
[39] A. P. Caffrey, P. E. Hopkins, J. M. Klopf *et al.*, Microscale Thermophys. Eng. **9**, 365 (2005).
[40] M. Pickel, A. B. Schmidt, F. Giesen, J. Braun, J. Minár, H. Ebert, M. Donath, and M. Weinelt, Phys. Rev. Lett. **101**, 066402 (2008).
[41] E. Carpene, E. Mancini, C. Dallera, M. Brenna, E. Puppin, and S. De Silvestri, Phys. Rev. B **78**, 174422 (2008).
[42] T. Greber, T. J. Kreutz, and J. Osterwalder, Phys. Rev. Lett. **79**, 4465 (1997).
[43] J. Fabian and S. Das Sarma, Phys. Rev. Lett. **81**, 5624 (1998).
[44] J. Walowski, G. Muller, M. Djordjevic, M. Münzenberg, M. Klaui, C. A. F. Vaz, and J. A. C. Bland, Phys. Rev. Lett. **101**, 237401 (2008).
[45] G. P. Zhang and W. Hubner, Phys. Rev. Lett. **85**, 3025 (2000).